*Sensors and Materials*, Vol. 38, No. 2 (2026) 679–684
MYU Tokyo



S & M 4337

# Optical, Electrical, and Scintillation Properties of Al-doped ZnO Films Synthesized by Laser-assisted CVD

Ryo Oi and Akihiko Ito*

Graduate School of Environment and Information Sciences, Yokohama National University,
79-7, Tokiwadai, Hodogaya-Ku, Yokohama, Kanagawa 240-8501, Japan

(Received October 31, 2025; accepted December 18, 2025)

***Keywords:*** Al-doped zinc oxide, CVD, transparent conductive oxides, luminescence, scintillation

We synthesized Al-doped ZnO (Al:ZnO) thin films by laser-assisted CVD and investigated their optical, electrical, and scintillation properties. The films exhibited a wurtzite-type ZnO structure with a strong (002) orientation. The averaged in-line transmittance in the visible wavelength region (380–780 nm) decreased from 90.4 to 49.0% as the Al concentration ($C_{Al}$) increased from 0 to 35.8 at.%. The sheet resistance reached a minimum of 2.47 Ω/sq at $C_{Al}$ = 7.9 at.%. The Al:ZnO films with $C_{Al}$ = 2.7–7.9 at.% exhibited UV emission at 375 nm originating from free excitons, whereas films with higher $C_{Al}$ showed no obvious emission. The average decay time constant of the Al:ZnO film with $C_{Al}$ = 7.9 at.% was 2.10 ± 0.08 ns under 5.5 MeV α-ray excitation. Moderate Al addition improved electrical conductivity and photoluminescence intensity, whereas excessive Al led to the deterioration of these properties owing to the formation of an amorphous phase.

## 1. Introduction

Zinc oxide (ZnO) is an abundant, low-cost, and nontoxic material that exhibits excellent optical and electrical properties and is therefore expected to have a wide range of applications. ZnO exhibits a high transmittance in the visible wavelength region (380–780 nm),[(1)] and by doping $Al^{3+}$ ions as a carrier source, a low resistivity of 4.8 Ω/sq can be achieved.[(2)] Consequently, ZnO is expected to be a promising alternative to indium tin oxide, which contains the rare metal indium, for use as a transparent conductive oxide in transparent electrodes of thin-film solar cells and touch panels. In addition, owing to its wide energy band gap (3.4 eV)[(3)] and near-band-edge UV emission (380 nm),[(4)] ZnO is also expected to be an alternative to gallium nitride for UV-light-emitting devices such as UV LEDs and laser diodes. Furthermore, ZnO is expected to be a potential scintillator material for α-ray detectors that convert incident α-rays into UV emission, and it can exhibit nano- and sub-nanosecond decay responses doped with $Al^{3+}$, $Ga^{3+}$, or $In^{3+}$ ions.[(5)]

Given these diverse potential advantages, extensive research has been conducted on ZnO, particularly in thin-film form. However, the suppression of crystal defects during synthesis

*Corresponding author: e-mail: ito-akihiko-xr@ynu.ac.jp
https://doi.org/10.18494/SAM6092

ISSN 0914-4935 
https://myukk.org/

remains a major challenge. Because ZnO is strongly ionic and has a low defect formation enthalpy, it tends to incorporate nonstoichiometric defects within its lattice, and oxygen vacancies and zinc interstitials are readily formed. These defects act as scattering centers for electrons, thereby degrading the electrical conductivity of the film. Moreover, zinc interstitials are known to cause blue emission around 480 nm, while oxygen vacancies are responsible for green emission near 530 nm.[6] Such defect-related emissions result in optical absorption in the visible range, reducing both transmittance and UV emission efficiency.

CVD is a process in which precursor gases are decomposed and reacted through chemical reactions to directly grow crystals on a substrate. In laser-assisted CVD, the reaction of precursor gases is induced by laser heating on the substrate surface, enabling the rapid synthesis of high-quality crystalline films.[7,8] Furthermore, by preparing the synthesis conditions, it allows the precise control of the film's crystal orientation and microstructure. In the present study, we synthesized Al-doped ZnO (Al:ZnO) films by laser-assisted CVD and investigated their optical and electrical properties and scintillation decay responses.

## 2. Materials and Methods

The laser-assisted CVD apparatus has been described elsewhere.[7] Metal–organic compounds of zinc bis(dipivaloylmethanate) (Strem Chemicals, USA) and aluminum tris(acetylacetonate) (Sigma-Aldrich, USA) were maintained at temperatures of 443 and 393–423 K, respectively, in precursor furnaces. The Al concentration in precursor vapor ($C_{Al}$) was varied from 2.7 to 35.8 at.%. The $C_{Al}$ molar ratio in the precursor vapor was estimated on the basis of the mass change in each precursor before and after deposition. The composition in the precursor gas often matches that in the film.[9] The resultant vapor was transferred to the CVD chamber using Ar carrier gas, and $O_2$ gas was separately introduced into the chamber through a double-tube nozzle. The total chamber pressure was maintained at 3 kPa. The quartz glass plate (5 mm × 5 mm × 0.5 $mm^t$) was used as a substrate. The substrate was heated by a $CO_2$ laser (wavelength: 10.6 μm; maximum laser output: 60 W; SPT Laser Technology, China) on a heating stage, and the deposition temperature was maintained at 767–813 K. Deposition was performed for 0.6 ks.

The phase composition of the resultant film was determined by X-ray diffraction (XRD; Bruker D2 Phaser, USA), and the optical transmittance was measured with an ultraviolet–visible spectrophotometer (JASCO V-630, Japan) in the wavelength range of 190–2500 nm. Photoluminescence (PL) and PL excitation (PLE) spectra were measured using a fluorescence spectroscopy spectrometer (JASCO FP-8300, Japan). The sheet resistance was measured with a digital multimeter (ADCMT 7461P, Japan).

Scintillation decay curves under 5.5 MeV α-ray excitation from an $^{241}Am$ source were measured using a photomultiplier tube (Hamamatsu Photonics R7600-200, Japan) and an oscilloscope (IWATSU ELECTRIC DS-5622A, Japan). The specimens were mounted on the window of the PMT with a thin layer of optical silicone grease (OHYO KOKEN KOGYO TSK5353, Japan).

## 3. Results and Discussion

Figure 1 shows the XRD patterns of the films synthesized at $C_{Al}$ = 2.7, 3.3, 7.9, 14.9, and 35.8 at.%. The XRD patterns were indexed as a (002)-oriented wurtzite-type ZnO phase (ICSD No. 44477). All the films deposited at $C_{Al}$ = 2.7–35.8 at.% were indexed with the (002)-oriented wurtzite-type ZnO phase, whereas the diffraction peaks became smaller and broader as $C_{Al}$ increased, implying amorphous or impurity phase segregation.

Figure 2 shows the in-line transmittance spectra and photographs of the Al:ZnO films grown on quartz glass substrate with various $C_{Al}$ values. The periodic undulations in the visible region (380–780 nm) were due to thin-film interference, suggesting that the Al:ZnO films synthesized in the present study were approximately 200–1000 nm thick. The average transmittances in the visible region were 70.4% for $C_{Al}$ = 2.7 at.%, 67.0% for $C_{Al}$ = 3.3 at.%, 57.1% for $C_{Al}$ = 7.9 at.%, 58.6% for $C_{Al}$ = 14.9 at.%, and 49.0% for $C_{Al}$ = 35.8 at.%. As $C_{Al}$ increased, the Al:ZnO films gradually became darker in appearance, accompanied by a gradual decrease in transmittance in the visible wavelength region [Figs 2(a')–2(e')]. This decrease was presumed to be caused by the formation of an amorphous phase in the films or free-carbon contamination from an $Al(acac)_3$ precursor due to excessive Al doping.[10] In the NIR wavelength region (1500–2500 nm), the transmittance decreased with increasing $C_{Al}$ [curves (a)–(c) in Fig. 2]. This decrease can be attributed to the increment of free carrier absorption due to the higher carrier concentration with $C_{Al}$,[11,12] while the amorphous phase formation at a high $C_{Al}$, as shown in Figs. 1(d) and 1(e), decreased the free carrier concentration and absorption at the near-infrared region [curves (d) and (f) in Fig. 2].

Table 1 shows the effects of $C_{Al}$ on the sheet resistance and scintillation decay time constant of the Al:ZnO films and the reported values. The sheet resistance of the Al:ZnO films decreased

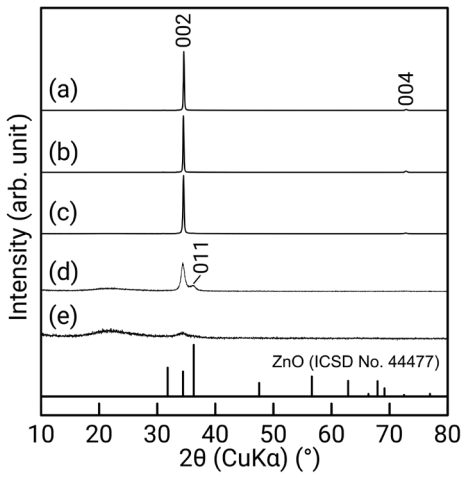


Fig. 1. XRD patterns of Al:ZnO films grown on quartz glass substrate at various $C_{Al}$ values: (a) 2.7, (b) 3.3, (c) 7.9, (d) 14.9, and (e) 35.8 at.%.

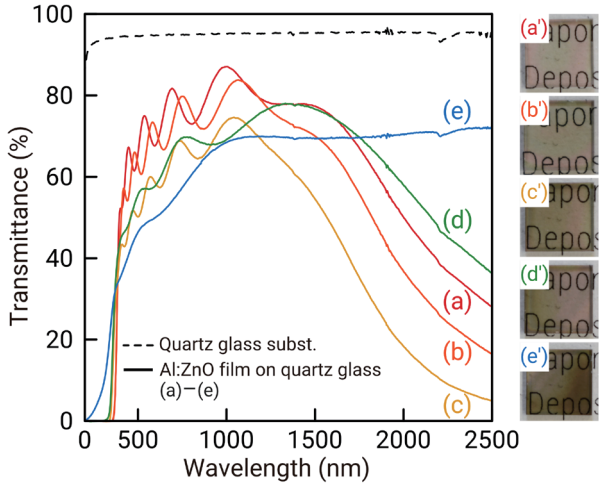


Fig. 2. (Color online) In-line transmittance spectra and photographs of Al:ZnO films with various $C_{Al}$ values: (a, a') 2.7, (b, b') 3.3, (c, c') 7.9, (d, d') 14.9, and (e, e') 35.8 at.%.

Table 1
Effects of $C_{Al}$ on the sheet resistance and decay time constant of the Al:ZnO films prepared in the present study and those reported in the literature.

| Synthesis method | Al concentration (at.%) | Sheet resistance (Ω/sq) | Decay time constant (ns) | Ref. |
|---|---|---|---|---|
| CVD | 2.7 | 24.3 | ** | (a)† |
| | 3.3 | 12.5 | ** | (b)† |
| | 7.9 | 2.5 | 2.10 ± 0.08 | (c)† |
| | 14.9 | * | ** | (d)† |
| | 35.8 | * | ** | (e)† |
| Sputtering | 4.3 | 4.9 | Not reported | Ref. 2 |
| Spray pyrolysis | 2.0 | 5.7 | Not reported | Ref. 13 |
| Hydrothermal | 1.0 | Not reported | 1.25 ± 0.12 | Ref. 5 |

*: outside the measurement range, **: not detected, †: present study

from 24.3 to 2.5 Ω/sq as $C_{Al}$ increased from 2.7 to 7.9 at.%, and the Al:ZnO films with $C_{Al}$ = 14.9–35.8 at.% were semiconducting or insulating (outside the measurement range). The tendency that there is an optimum amount of Al doping for improving electrical conductivity was consistent with the literature values for Al:ZnO films prepared by sputtering and spray pyrolysis (as listed in Table 1).[2,13] Al doping in ZnO increased the carrier concentration and improved the electrical conductivity, whereas excessive Al doping generated additional carrier scattering centers, reducing the carrier mobility.[10,14]

Figure 3 shows the effects of $C_{Al}$ on the PL spectra of the Al:ZnO films excited at 350 nm. The Al:ZnO films with $C_{Al}$ = 2.7–7.9 at.% exhibited UV emission peaking at 375 nm, which was attributed to the radiative recombination of free excitons.[15,16] Al doping suppressed the defect-induced deep-level blue and green emissions peaking at 480 and 530 nm, respectively, because the replacement of $Zn^{2+}$ sites within the ZnO lattice by $Al^{3+}$ ions, which exhibit a larger valence and a smaller ionic radius, reduced the number of oxygen vacancies and interstitial zinc atoms.[17] The UV emission intensity increased as $C_{Al}$ increased from 2.7 to 7.9 at.%, whereas the Al:ZnO films with $C_{Al}$ = 14.9–35.8 at.% showed no obvious UV emission in their PL spectra. This may be attributed to excess Al incorporation, which caused lattice strain and amorphous phase segregation, shown as XRD peak broadening in Figs. 1(d) and 1(e), thereby suppressing the PL emissions.

Scintillation decay curves under 5.5 MeV α-ray radiation from the $^{241}$Am source were measured for Al:ZnO films. Only the Al:ZnO film with $C_{Al}$ = 7.9 at.%, which exhibited the highest PL intensity, yielded a measurable decay response for α-rays. According to the SRIM simulation,[18] the Al:ZnO thin film, for example, with a thickness of 500 nm, absorbs only about 1% of the α-ray energy. Thus, even for other Al:ZnO films where PL could be measured, the small film thickness resulted in insufficient scintillation, making it difficult to distinguish from the PMT thermal noise (decay time constant of 1.73 ± 0.01 ns). The decay curves were collected by excluding PMT thermal noise. Figure 4 shows the scintillation decay curve of the Al:ZnO film with $C_{Al}$ = 7.9 at.% under 5.5 MeV α-ray excitation from the $^{241}$Am source. Assuming that the measured decay curve can be represented as the convolution of an instrument response factor approximated by a Gaussian function and the exponential decay, the measured scintillation decay curves were fitted by an exponentially modified Gaussian function,[19]

$$\mathrm{EMG}(t) = h\sigma\sqrt{2\pi}/(2\tau)\exp\left[(t_0 - t)/\tau + \sigma^2/(2\tau^2)\right]\left\{|\tau|/\tau - \mathrm{erf}\left[(t_0 - t)/\sqrt{2}\sigma + \sigma/\sqrt{2}\tau\right]\right\}, \quad (1)$$

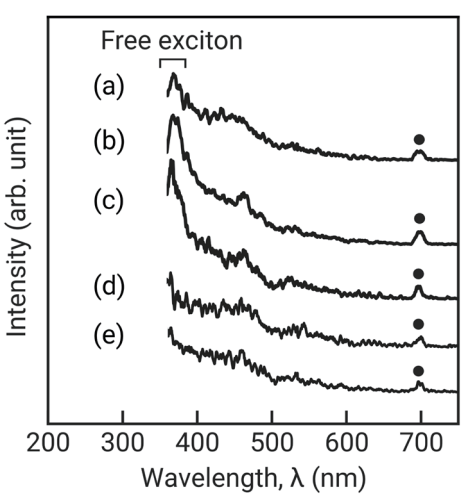


Fig. 3. Effects of $C_{Al}$ on PL emission spectra excited at $\lambda_{ex}$ = 350 nm for Al:ZnO films grown at various $C_{Al}$ values: (a) 2.7, (b) 3.3, (c) 7.9, (d) 14.9, and (e) 35.8 at.%. Filled circles indicate the second harmonic of the excitation light.

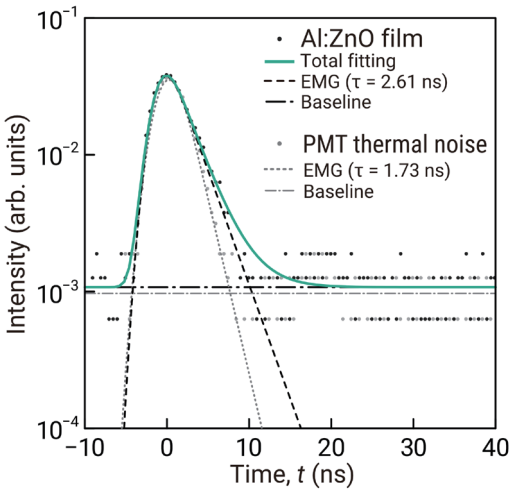


Fig. 4. (Color online) Scintillation decay curve under 5.5 MeV α-ray irradiation from $^{241}$Am source for the Al:ZnO film grown at $C_{Al}$ = 7.9 at.%. Dots indicate measured data, and solid, dashed, dotted, and single-dot chain lines indicate fitting curves.

where $h$, $t_0$, and $\sigma$ are the Gaussian height, center, and width, respectively, and $\tau$ denotes a decay time constant. The total fitting model is the sum of the EMG($t$) function and a constant for the baseline. The decay curve was fitted using the Fityk software[20] with $h$ = 0.06, $t_0$ = −1.39, $\sigma$ = 1.29, and $\tau$ = 2.61 (solid line in Fig. 4), and the average decay time constant of the Al:ZnO film at $C_{Al}$ = 7.9 at.% was 2.10 ± 0.08 ns.

Yanagida and coworkers reported that ZnO film and bulk crystal had decay time constants of 0.60 ns for α-ray excitation and 4.3 ns for X-ray excitation.[15,21] Masai *et al.* reported that ZnO crystallites precipitated in a glass matrix had fast decay time constants of 1.7–1.8 ns for X-ray excitation.[16] Kurudirek *et al.* reported that the cathode luminescence decay time constants of ZnO and Al:ZnO films were 0.57 and 1.25 ns, respectively.[5] Thus, since the decay time constant of nondoped ZnO has been reported to have values in the nanosecond range, and since a slight increase in decay time constant due to Al doping has also been reported, the decay time constant of the Al:ZnO film synthesized in the present study was determined to be 2.10 ns.

## 4. Conclusions

Al:ZnO films were synthesized by laser-assisted CVD at various $C_{Al}$ values of 2.7–35.8 at.%. All the films exhibited the wurtzite-type ZnO phase with a strong preferred (002) orientation. The optical transmittance in the visible region gradually decreased with increasing $C_{Al}$, which was attributed to amorphous phase formation and residual carbon incorporation caused by excessive Al doping. The sheet resistance reached a minimum of 2.5 Ω/sq at $C_{Al}$ = 7.9 at.%, indicating the increase in carrier concentration due to $Al^{3+}$ substitution for $Zn^{2+}$ in the ZnO lattice, whereas further Al addition led to a loss of electrical conductivity owing to the formation

of an amorphous phase and defect centers. The PL spectra showed UV emission at 375 nm for $C_{Al}$ = 2.7–7.9 at.%, and the intensity increased with Al concentration. However, no obvious UV emission was observed at $C_{Al}$ = 14.9–35.8 at.% owing to amorphous phase formation induced by excessive Al incorporation. Under 5.5 MeV α-ray excitation, the scintillation decay time constant of the Al:ZnO film with $C_{Al}$ = 7.9 at.% was measured to be 2.10 ± 0.08 ns.

## Acknowledgments

This study was supported in part by JSPS KAKENHI Grant Numbers 21H05199, 24K91211, 24K21685, 24K21746, and 25H00796.

## References

1 B. C. Jiao, X. D. Zhang, C. C. Wei, J. Sun, Q. Huang, and Y. Zhao: Thin Solid Films **520** (2011) 1323. https://doi.org/10.1016/j.tsf.2011.04.152
2 N. Hirahara, B. Onwona-Agyeman, and M. Nakao: Thin Solid Films **520** (2012) 2123. https://doi.org/10.1016/j.tsf.2011.08.100
3 P. Camarda, F. Messina, L. Vaccaro, S. Agnello, G. Buscarino, R. Schneider, R. Popescu, D. Gerthsen, R. Lorenzi, F. M. Gelardi, and M. Cannas: Phys. Chem. Chem. Phys. **18** (2016) 16237. https://doi.org/10.1039/C6CP01513A
4 X. Liu, X. Wu, H. Cao, and R. P. H. Chang: J. Appl. Phys. **95** (2025) 3141. https://doi.org/10.1063/1.1646440
5 M. Kurudirek, S. V. Kurudirek, A. Erickson, N. Hertel, B. J. Lawrie, Y. Tratsiak, B. Klein, C. L. Melcher, C. J. Summers, and P. J. Sellin: Discov. Nano **20** (2025) 109. https://doi.org/10.1186/s11671-025-04227-5
6 H. Zeng, G. Duan, Y. Li, S. Yang, X. Xu, and W. Cai: Adv. Funct. Mater. **20** (2010) 561. https://doi.org/10.1002/adfm.200901884
7 A. Ito: J. Ceram. Soc. Jpn. **129** (2021) 646. https://doi.org/10.2109/jcersj2.21135
8 S. Matsumoto, A. Minamino, and A. Ito: Sens. Mater. **33** (2021) 2209. https://doi.org/10.18494/SAM.2021.3325
9 S. Matsumoto and A. Ito: J. Ceram. Soc. Jpn. **129** (2021) 1. https://doi.org/10.2109/jcersj2.20156
10 M. W. Zhu, H. B. Ma, P. H. Jin, Y. N. Jin, N. Jia, H. Chen, and C. Z. Liu: Appl. Phys. A **126** (2020) 484. https://doi.org/10.1007/s00339-020-03670-8
11 V. Sittinger, F. Ruske, A. Pflug, W. Dewald, B. Szyszka, and G. Dittmar: Thin Solid Films **518** (2010) 3115. https://doi.org/10.1016/j.tsf.2009.09.167
12 C. Agashe, O. Kluth, G. Schöpe, H. Siekmann, J. Hüpkes, and B. Rech: Thin Solid Films **442** (2003) 167. https://doi.org/10.1016/S0040-6090(03)00966-0
13 W. Sripianem, A. Chuchuay, P. Kiatthanabumrung, N. Saengow, T. Na Wichean, S. Jongthammanurak, P. Jantaratana, and R. Techapiesancharoenkij: Mater. Today Proc. **5** (2018) 9519. https://doi.org/10.1016/j.matpr.2017.10.133
14 J. S. Bhat, A. S. Patil, N. Swami, B. G. Mulimani, B. R. Gayathri, N. G. Deshpande, G. H. Kim, M. S. Seo, and Y. P. Lee: J. Appl. Phys. **108** (2010) 043513. https://doi.org/10.1063/1.3452333
15 T. Yanagida, Y. Fujimoto, K. Yamanoi, M. Kano, A. Wakamiya, S. Kurosawa, and N. Sarukura: Phys. Status Solidi C **9** (2012) 2284. https://doi.org/10.1002/pssc.201200176
16 H. Masai, T. Yanagida, and T. Fujiwara: Sens. Mater. **27** (2015) 237. https://doi.org/10.18494/SAM.2015.1088
17 B. Tönbül, H. A. Can, T. Öztürk, and H. Akyıldız: Mater. Sci. Semicond. Process. **127** (2021) 105735. https://doi.org/10.1016/j.mssp.2021.105735
18 J. F. Ziegler, M. D. Ziegler, and J. P. Biersack: Nucl. Instrum. Methods B **268** (2010) 1818. https://doi.org/10.1016/j.nimb.2010.02.091
19 T. Nakayama, S. Kurosawa, and A. Ito: J. Lumin. **288** (2025) 121589. https://doi.org/10.1016/j.jlumin.2025.121589
20 M. Wojdyr: J. Appl. Crystallogr. **43** (2010) 1126. https://doi.org/10.1107/S0021889810030499
21 T. Yanagida, N. Kawaguchi, Y. Fujimoto, Y. Yokota, T. Tokutake, M. Miyamoto, H. Sekiwa, J. Kobayashi, V. Chani, and A. Yoshikawa: Jpn. J. Appl. Phys. **50** (2011) 01BG06. https://doi.org/10.1143/JJAP.50.01BG06